RS-8232-2/ 70176

8524

8232-2//070176

00000001 -

SAND88-0633
Unlimited Release
Printed February 1990

Initial Structural Response Measurements and Model Validation for the Sandia 34–Meter VAWT Test Bed

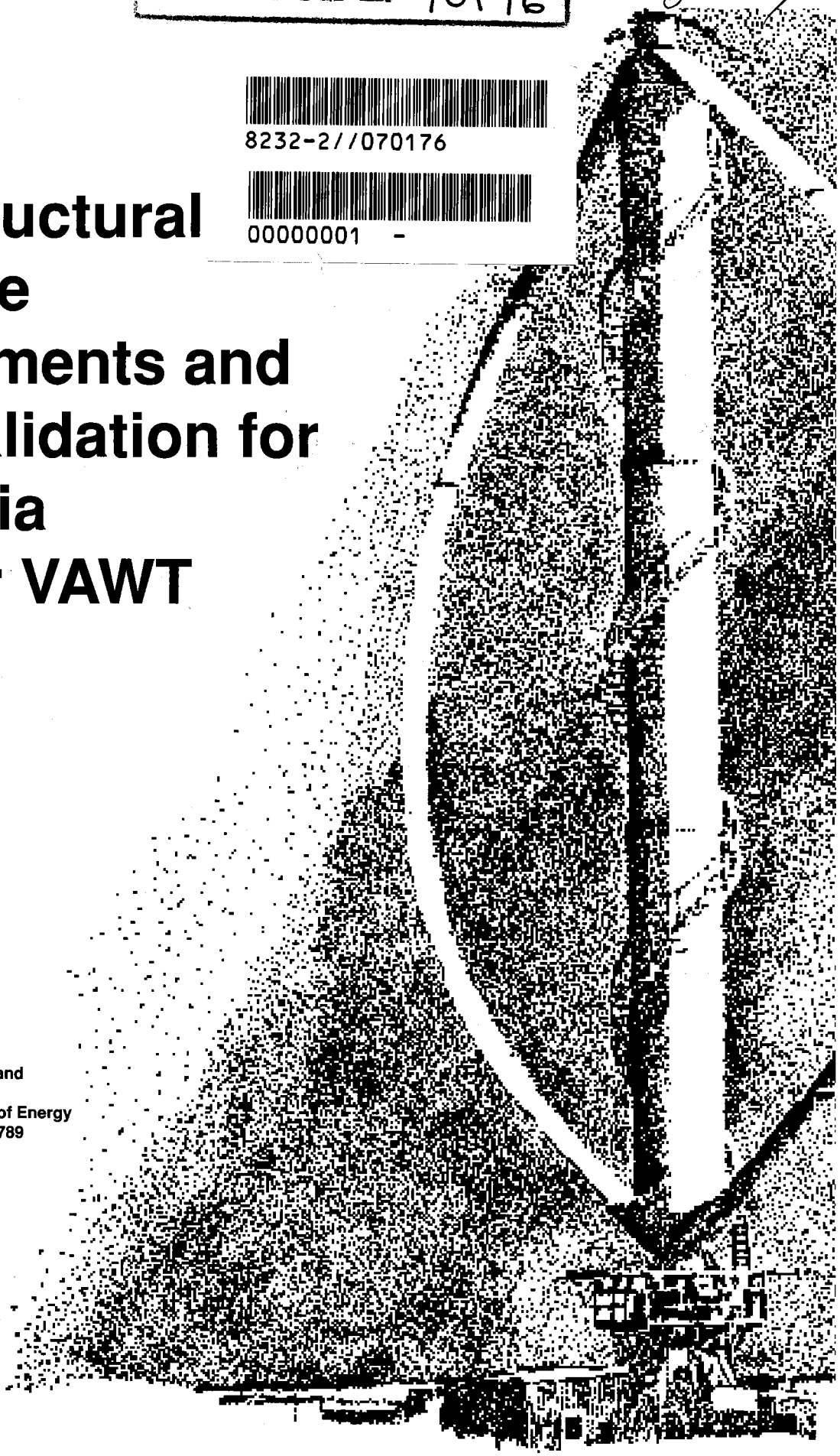

T.D. Ashwill

Prepared by
Sandia National Laboratories
Albuquerque, New Mexico 87185 and
Livermore, California 94550
for the United States Department of Energy
under Contract DE-ACO4-76DP00789

Issued by Sandia National Laboratories, operated for the United States Department of Energy by Sandia Corporation.

NOTICE: This report was prepared as an account of work sponsored by an agency of the United States Government. Neither the United States Government nor any agency thereof, nor any of their employees, nor any of their contractors, subcontractors, or their employees, makes any warranty, express or implied, or assumes any legal liability or responsibility for the accuracy, completeness, or usefulness of any information, apparatus, product, or process disclosed, or represents that its use would not infringe privately owned rights. Reference herein to any specific commercial product, process, or service by trade name, trademark, manufacturer, or otherwise, does not necessarily constitute or imply its endorsement, recommendation, or favoring by the United States Government, any agency thereof or any of their contractors or subcontractors. The views and opinions expressed herein do not necessarily state or reflect those of the United States Government, any agency thereof or any of their contractors.

Printed in the United States of America. This report has been reproduced directly from the best available copy.

Available to DOE and DOE contractors from
Office of Scientific and Technical Information
PO Box 62
Oak Ridge, TN 37831

Prices available from (615) 576-8401, FTS 626-8401

Available to the public from
National Technical Information Service
US Department of Commerce
5285 Port Royal Rd
Springfield, VA 22161

NTIS price codes
Printed copy: A02
Microfiche copy: A01

Distribution
Category
UC-261

SAND88-0633
Unlimited Release
Printed February 1990

INITIAL STRUCTURAL RESPONSE MEASUREMENTS AND MODEL VALIDATION FOR THE SANDIA 34-METER VAWT TEST BED

Thomas D. Ashwill
Wind Energy Research Division
Sandia National Laboratories
Albuquerque, New Mexico 87185

ABSTRACT

Sandia National Laboratories (SNL) has designed and constructed a 34-meter diameter vertical axis wind turbine (VAWT) Test Bed. The machine will be used to advance research in aerodynamics and structural dynamics, improve fatigue life prediction capabilities, and investigate control algorithms and system concepts. The Test Bed has extensive instrumentation including 70 strain gauges to measure blade and tower response. Immediately after the blades were mounted, blade gravity stresses were measured and a modal test on the stationary rotor performed to determine zero rpm modal frequencies. Assembly and start-up tests are complete, and testing is in the machine characterization phase. Structural resonance surveys will fully characterize the modal frequencies and mode shapes of the rotor, drive train and guy cables. Measured gravity stresses, centrifugal stresses, and modal frequencies are compared to predicted values.

INTRODUCTION

The 34-m VAWT Test Bed is a variable-speed, research turbine recently designed and constructed by Sandia National Labs. The design of this 500 kW machine incorporates the results of recent VAWT research in aerodynamics and structural dynamics. The turbine will be used to evaluate the advances in these areas and to contribute to developments in other areas such as fatigue life predictive techniques, stochastic wind modeling, variable-speed control algorithms, and system design concepts. The construction of the Test Bed, which is located at the U.S.D.A. Agricultural Research Service facility, 15 miles west of Amarillo, Texas, has been completed, and testing is underway. The blades were mounted on the tower in November, 1987, and the first rotation with blades occurred on February 4, 1988.

Assembly and start-up tests, Phase I of the Test Plan (1), are finalized. Phase I included testing of the power system and controller, verification of the blade strain gauges, testing of the transmission and drive train for vibrations and power losses, set-up and checkout of the brake system and implementation of the data acquisition system. Immediately after the blades were mounted, blade gravity stresses were measured and a modal test performed on the stationary rotor. The modal test measured stationary modal frequencies, which have been compared to predicted frequencies. This allows the predicted fanplot (a plot of modal frequencies versus rotation rate) to be used more accurately as a guide for identifying resonant frequencies during rotation and provides validation of the finite element model used to obtain the predictions.

The turbine testing has progressed into the machine characterization phase - Phase II of the Test Plan. This testing will determine the structural response and aerodynamic performance over the entire operating range. It will include further evaluation of the variable speed controller, understanding its capabilities, and upgrading the control algorithm to reflect knowledge gained during the characterization. Before running for long periods of time at different rotation rates and wind speeds, a resonance survey was conducted by operating for short periods at several rotation rates from 6 through 40 rpm in low, medium, and high wind conditions. This survey characterizes the modal frequencies of the rotor, drive train, and guy cables and allows for the determination of mean stress levels and approximate cyclic stress levels. The evaluation of structural response and turbine performance during these short periods has been followed by operation for longer periods of time to collect enough time series records to create statistically reliable, averaged data (2).

This report describes the major aspects of the measured structural response data obtained up to and including the resonance surveys. (The turbine has rotated from 6 to 40 rpm in winds up to 17 mps). After a general description of the Test Bed structure and the finite element model employed in the structural design, measurements of gravity stresses, centrifugal stresses, and modal frequencies are shown and compared to predicted values.

GENERAL DESCRIPTION OF THE TEST BED

The 34-meter Test Bed is rated at 500 kW at 37.5 rpm in a 12.8 mps (28 mph) wind. Figure 1 shows a photograph of the turbine in its completed form. The rotor is 34 meters (110 feet) in diameter and has a height-to-diameter ratio of 1.25. The turbine, which has a total height of 50 meters (165 ft), is supported at the top by three sets of double guy cables each of which is 63.5 mm (2 1/2 in.) in diameter. Each cable pair is tensioned to 826 kN (186,000 lb) and is anchored at ground level to a reinforced concrete tiedown block measuring 4.3x4.3x6.1 m^3 (14x14x20 ft^3). The tower, or column, is an aluminum cylinder, 3 meters (10 ft) in diameter, constructed of 13 mm (0.5 in.) rolled plates, butt-welded together. Two blade mounts attached to the tower at each end are box-like structures that provide blade attachment surfaces and transition the tower diameter down to bearing shaft diameters.

Each blade is step-tapered with five sections constructed of extruded 6063-T6 aluminum. The top and bottom root sections are straight with a 1.22 meter (48 in.) chord using a NACA 0021 profile. The equatorial section, with a 17.1 meter (675 in.) radius of curvature, has a 0.91 meter (36 in.) chord with an SNLA 0018/50 profile. The intermediate sections, with a 30.0 meter (1180 in.) radius of curvature, have a 1.07 meter (42 in.) chord with an SNLA 0018/50 profile. The SNLA 0018/50 airfoils are part of a series of natural laminar flow airfoils developed at Sandia specifically for use on VAWT's (3). Because all three chords are too large to be fabricated from a single extrusion, each blade section is made of two or three single extrusions bolted together in the spanwise direction. The seven different extrusions that make up the three profiles were successfully extruded to specification during October, 1986 by Consolidated Aluminum, Inc. of Madison, Illinois. The 36-inch and 42-inch chord sections were bent to the proper radius around dies designed specifically for the Test Bed. The extrusion-to-extrusion bolts were retorqued to specification after the blade bending. The extrusion-to-extrusion assembly and blade bending process were performed by Flow Industries of Kent, Washington.

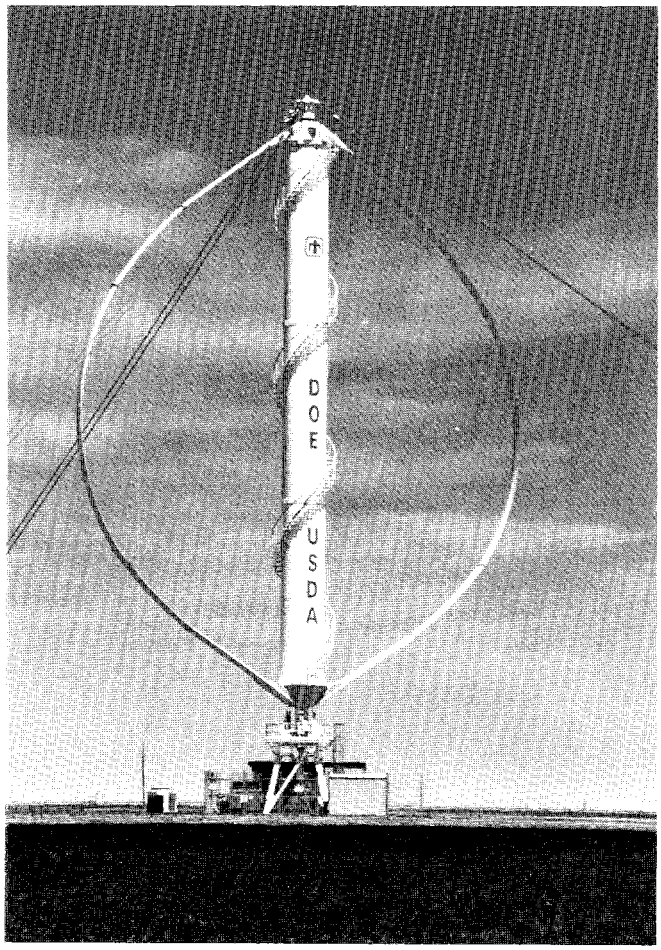

Fig. 1. 34-Meter Test Bed

The blade shape approximates a 37.5 rpm troposkien and contains "kinks", or slope discontinuities, of 6-7 degrees at the blade-to-blade joints as shown in Fig. 2, a schematic of the blade shape geometry. Because of the multi-sectioned, step-tapered characteristics of the Test Bed blades, the normally-used straight/single-curve/straight approximation to a troposkien was not employed. A better approximation resulted by implementing the different radii of curvature along the blade and the slope discontinuities at the blade joints where mass is concentrated. Design calculations (4) show that these implementations reduce the largest mean flatwise stresses approximately fifty percent. This mean stress reduction extends the estimated fatigue life by a factor of two to four.

THE FINITE ELEMENT MODEL

The structural design process (5) of the Test Bed incorporated the finite element code NASTRAN to determine the turbine dynamic response. Gravity stresses were also predicted with NASTRAN using a static solution (Rigid Format 24). Predicted modal frequencies were computed with NASTRAN using an eigenvalue solution methodology (FEVD) developed at Sandia (6). In this methodology the stiffness matrix, representing the turbine structure when subjected to centrifugal and gravitational loading, is determined by running a series of geometric nonlinear analyses (Solution 64). The complex eigenvalue analysis (Solution 67) is then used after including rotating coordinate system effects (Coriolis and softening matrices). The mean stresses due to gravitational and centrifugal loading at a particular rpm are output by Solution 64. The complex mode shapes and their respective frequencies of vibration are determined by Solution 67.

A forced response analysis code, called FFEVD (7), determines the vibratory stresses. In FFEVD the stiffness, Coriolis and softening matrices are computed just as in FEVD and input to the complex frequency response analysis (Solution 68) along with the steady (per-rev) wind loads determined by the double streamtube code CARDAA (8). Solution 68 then computes the structural response at each per-rev frequency.

Figure 3 shows the finite element grid for the 34-m Test Bed. It consists of 42 CBEAM elements for each blade, 25 CBEAM elements for the tower, and 2 CBEAM's for each of the four "mini-struts." (The NASTRAN beam element, CBEAM, has properties that include two-dimensional bending, extension, and torsion.) These ministruts model the large blade mounts. The guy cables that restrict motion at the top of the turbine are represented by two orthogonal, horizontal springs, a torsional spring, and a

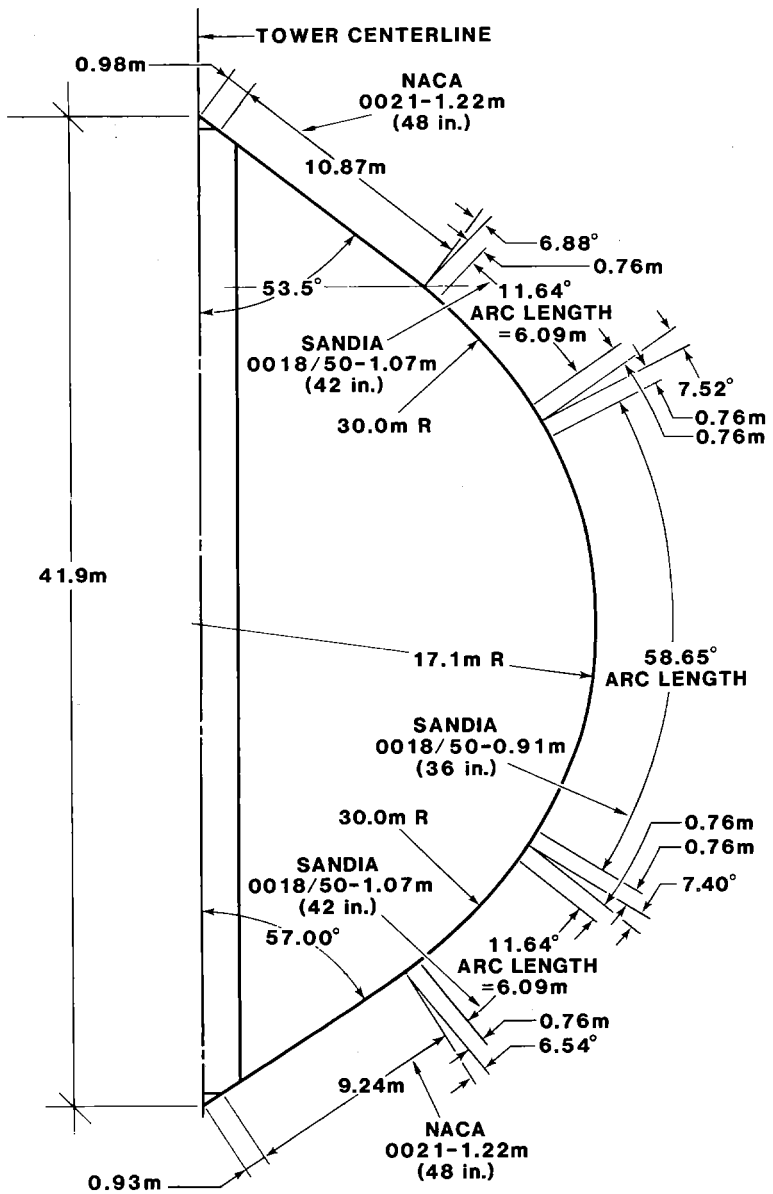

Fig. 2. Blade Shape Geometry

vertical load acting down through the tower. At the bottom of the rotor, at grid point 1, the restriction of motion by the support stand is represented by two orthogonal, horizontal springs. A torsional spring at grid point 1 represents the torsional stiffness of the drive train. Concentrated masses are added at several grid points along the tower to account for the entire tower mass. The mass of the blade joints is distributed evenly along the relatively short joint elements. As the turbine was constructed, each component was measured and weighed. The concentrated masses and properties of the finite elements were then updated in the model to reflect these "as-built" conditions.

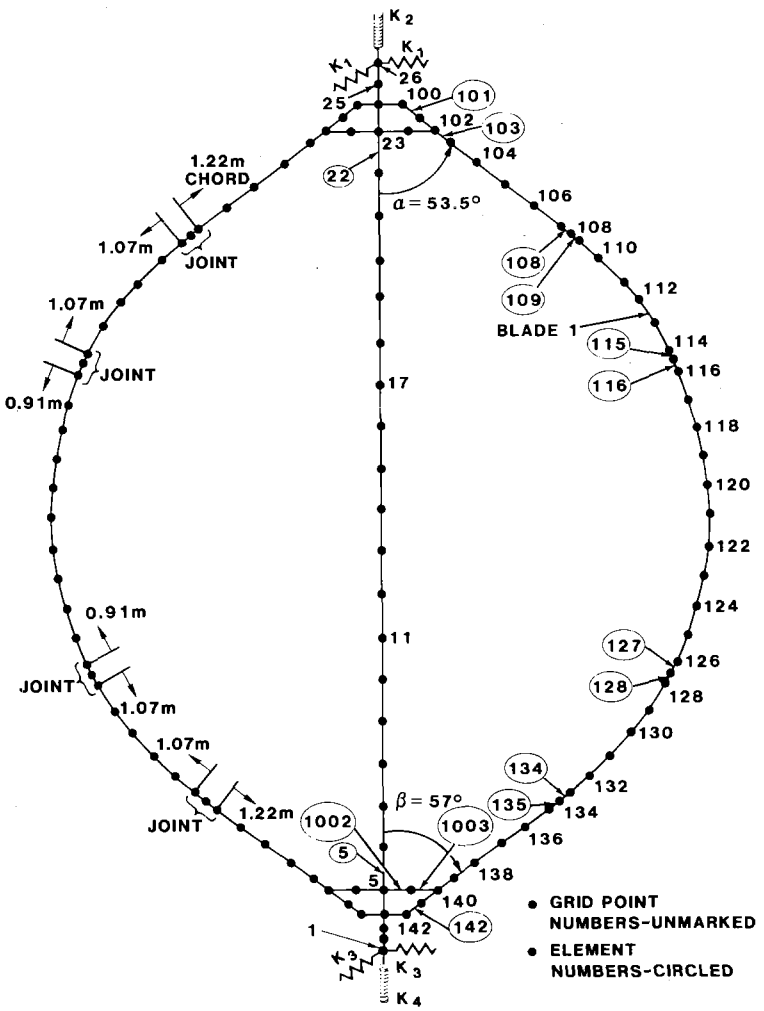

Fig. 3. Finite Element Grid

For blade one, elements 101-108 and 135-142 represent the blade root sections, elements 109-115 and 128-134 the intermediate sections, and elements 116-127 the equatorial section. Blade two is identical in structure to blade one. For comparisons with test results, an additional boundary condition was added to the model at grid point 2 to represent the brakes in the engaged condition. This condition was modelled as two orthogonal, horizontal springs and a torsional spring (torsion about the vertical axis) equal to the appropriate stiffnesses of the support stand.

GRAVITY STRESSES

The Test Bed has been instrumented with 70 strain gauges that measure axial, lead-lag, and flatwise response in the blades and torque and bending in the tower (9). Brake strain gauges and damage gauges that measure crack growth of a pre-cracked aluminum coupon also have been installed. When the blades were first instrumented, the flatwise gauges were validated by hanging known weights from each blade section, recording the strains and comparing them to calculations. The entire set of gauges functioned correctly, and the measured strains agreed with predictions to within 2 percent. Following the gauge validation tests, the blade sections were transported to the turbine site and bolted together while at the same time pulling instrumentation cabling through two blade cavities. The blade cavities containing the cabling were filled with structural foam to prevent cable movement. Before the blades were mounted, the gauges were rechecked, recalibrated and rezeroed. Immediately after the blades were mounted, the gauges were monitored to measure gravity strains.

Figure 4 compares the measured flatwise gravity stresses to the predictions. Stresses along the blade from the top to the bottom are plotted left to right on the x-axis. Positive stress corresponds to tension on the outside of the blade. The patterns of stress distribution for the measured and predicted are very similar; the values agree well at the ends of the blades where fatigue is a major concern. Discontinuities in the stress distribution occur at the joints because of the change of blade stiffness at those locations. The analytical values show an offset along the middle portion, however, indicating an underprediction at the tension side and an overprediction at the compression side of up to 10 MPa (1440 psi). This is also the area where the only significant differences between blades one and two occur. These differences may be due to small errors in the blade shape geometry in the model. Gravity stresses are especially sensitive to small angle changes at the blade-to-tower connection. The blade section lengths were carefully measured in

the field, and the blade sections (including the instrumentation cabling, paint and aerodynamic smoothing compound) were weighed several times. A survey of the turbine structure will be performed to attempt to determine the exact "as-mounted" blade attachment angles.

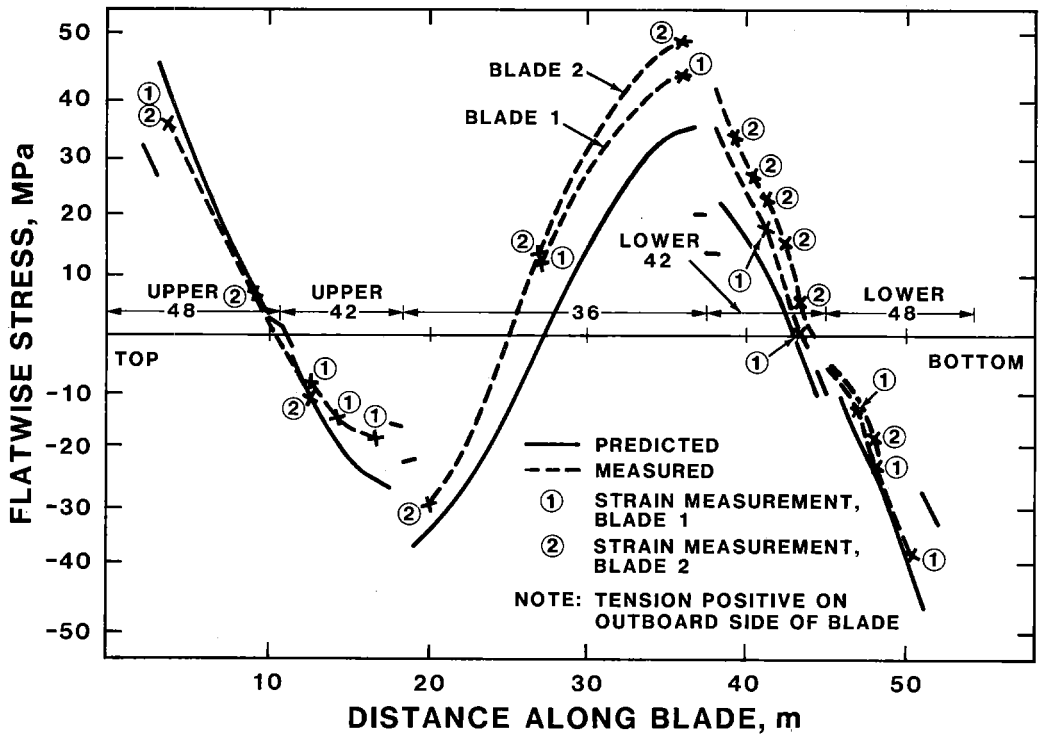

Fig. 4. Flatwise Gravity Stress Distribution

MODAL FREQUENCIES

After the blades were mounted on the tower, a modal test was performed on the stationary rotor by Sandia's Modal and Structural Mechanics Division (7544). During this test, frequency response functions were measured using both wind and step relaxation (snap releasing) excitations. Accelerometers were temporarily attached to the blades, tower and cables. These measurements were used to determine the mode shapes, their frequencies of vibration, and modal damping values. Reference 10 describes the details of the Test Bed modal test.

Table I compares the measured modal frequencies with those determined analytically. The mode number and name are listed in the first two columns (Figure 5 shows the shapes of these modes when viewed from three orthogonal directions). Columns three and four of Table I show the modal frequencies for the stationary rotor measured after a snap release and during wind excitation, respectively. Column five lists the predicted values, and column six lists measured frequencies obtained from amplitude spectra plots of strain gauge data taken during the the wind-excited modal analysis. There is excellent agreement between the measured and predicted frequencies for the first eleven modes. At the higher modes the predicted modal frequencies do not agree as well with the measurements. The two- dimensional finite element model appears to have a limit on its ability to predict these higher modes. However, in general, the higher modes have lower deformation and less energy associated with them.

Mode Number	Mode Shape	Modal Analysis: Snap Release	Modal Analysis: Wind Excitation	Predicted	Strain Gauge Spectra
1	1FA-First Flatwise Antisymmetric	1.04	1.06	1.05	1.06
2	1FS-First Flatwise Symmetric	1.04	1.06	1.05	
3	1Pr First Propeller (Rotor Twist)	1.35	1.52	1.56	1.50
4	1B-First Blade Edgewise	1.81	1.81	1.72	1.82
5	2FA-Second Flatwise Antisymmetric	2.06	2.06	2.07	2.14
6	2FS-Second Flatwise Symmetric	2.16	2.16	2.14	
7	1TI-First Tower In-Plane	2.49	2.50	2.46	2.50
8	1TO-First Tower Out-of-Plane	2.60	2.61	2.58	2.61
9	3FA-Third Flatwise Antisymmetric	3.45	3.50	3.49	3.51
10	3FS-Third Flatwise Symmetric	3.45	3.50	3.51	
11	2Pr Second Propeller	3.59	3.59	3.52	3.59
12	2B-Second Blade Edgewise	-	4.06	3.90	4.05
13	2TI-Second Tower In-Plane	-	4.69	4.33	-
14	2TO-Second Tower Out-of-Plane	-	-	4.57	-
15	4FS-Fourth Flatwise Symmetric	-	5.09	5.25	-
16	4FA-Fourth Flatwise Antisymmetric	-	5.30	5.37	-
17	3Pr Third Propeller	-	-	5.71	-

Table I. Stationary Modal Frequencies - Brakes Engaged

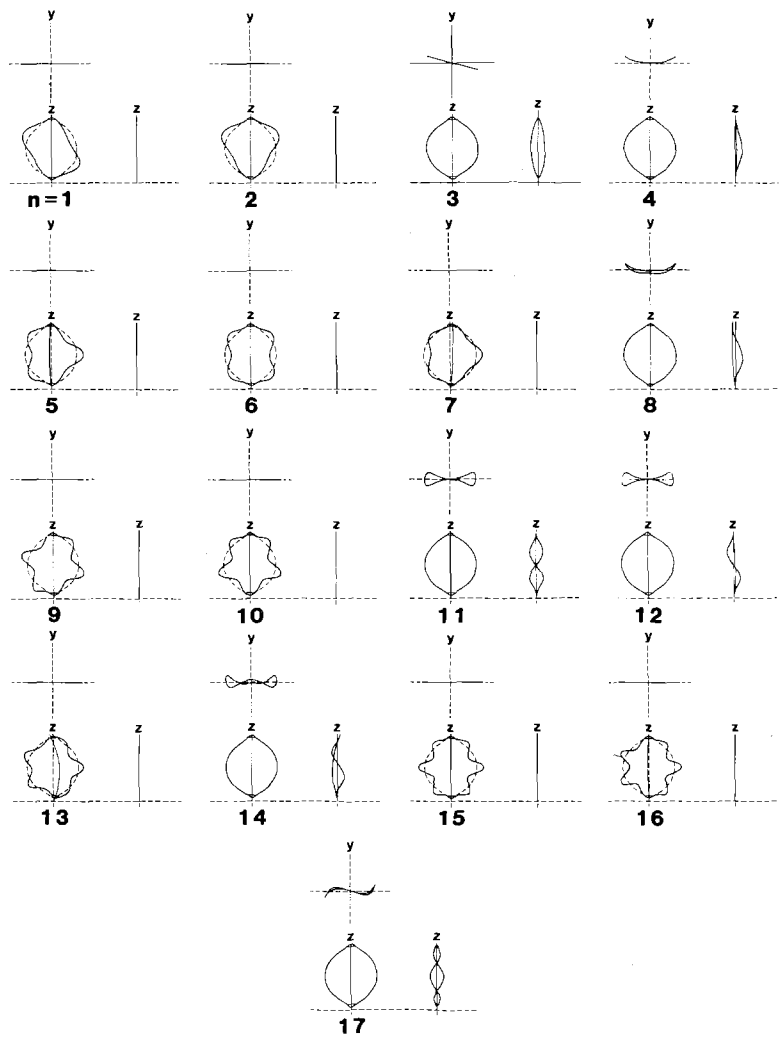

Fig. 5. Mode Shapes

The first propeller mode is approximately 1.5 Hz with the brakes engaged and 0.2 Hz with the brakes released. By adding or changing elastomeric pads (known as hockey pucks because of their size and shape), the drive train stiffness can be adjusted and the frequency of the first propeller mode changed. The first three flatwise modes (both antisymmetric and symmetric), the first tower in-plane and out-of-plane modes, and the second propeller mode were all predicted within two percent of the measured frequencies. The first blade edgewise mode is underpredicted by 0.09 Hz (approximately 5 percent) indicating that the blades are actually slightly stiffer in the lead-lag direction than modeled or that the blade-to-tower attachment should be more rigid in that direction. The close agreement between predicted and measured frequencies for the first eleven modes is an indication that the finite element model does an excellent job in representing the Test Bed - a complicated three-dimensional structure.

The measured frequencies resulting from the two methods of excitation - snap releasing and wind excitation - are very close. Only the first propeller mode shows any significant difference in frequency between the two methods. The reason for this difference is not clear. However, the snap release puts more energy into the system and possibly alters the brake boundary condition slightly. As shown in column six, the peak frequencies from the strain amplitude spectra agree closely with those measured by the modal test.

The first two guy cable frequencies, modes n=1 and n=2, were designed to vibrate at 0.81 Hz and 1.62 Hz, respectively, at a nominal cable tension of 826 kN (186,000 lb), assuming a uniform cross-sectional area the entire cable length. This design puts the first cable mode below 2P (two per-rev) and the second mode between 2P and 4P for the entire operating range. The first four cable frequencies were measured at 0.81, 1.27, 2.05, and 3.02 Hz. The first cable mode occurs at the frequency to which it was designed (0.81 Hz), however, the second measured mode is significantly lower than the second design mode. This is due to an interaction between the cables and heavy cable attachment hardware at the lower cable connection. There is much less motion associated with this mode than the n=1 mode. As the cable fanplot (Fig. 6) indicates, this resonance is the second mode crossing the 2P line. A new guy cable model that includes the ability to model the variation in mass distribution has recently been developed and correctly predicts the four measured cable modes.

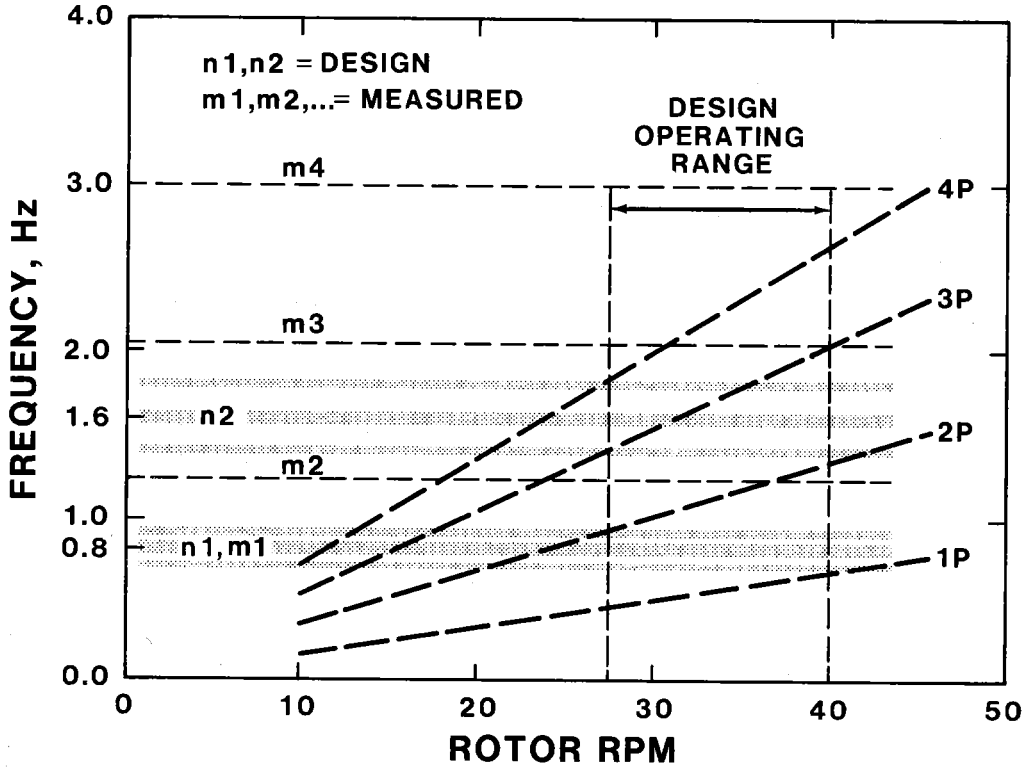

Fig. 6. Cable Fanplot

The predicted fanplot for the "as-built" finite element model with the brakes released is shown in Fig. 7. Because the brake boundary condition is eliminated, some of the stationary tower modal frequencies, as expected, are lower than the modal frequencies shown in Table I. The blade modal frequencies are not affected by this boundary condition. Because potential resonances are possible wherever a modal frequency crosses a per-rev line, both this rotor fanplot and the guy cable fanplot have been employed extensively during the resonance surveys to identify and avoid resonances.

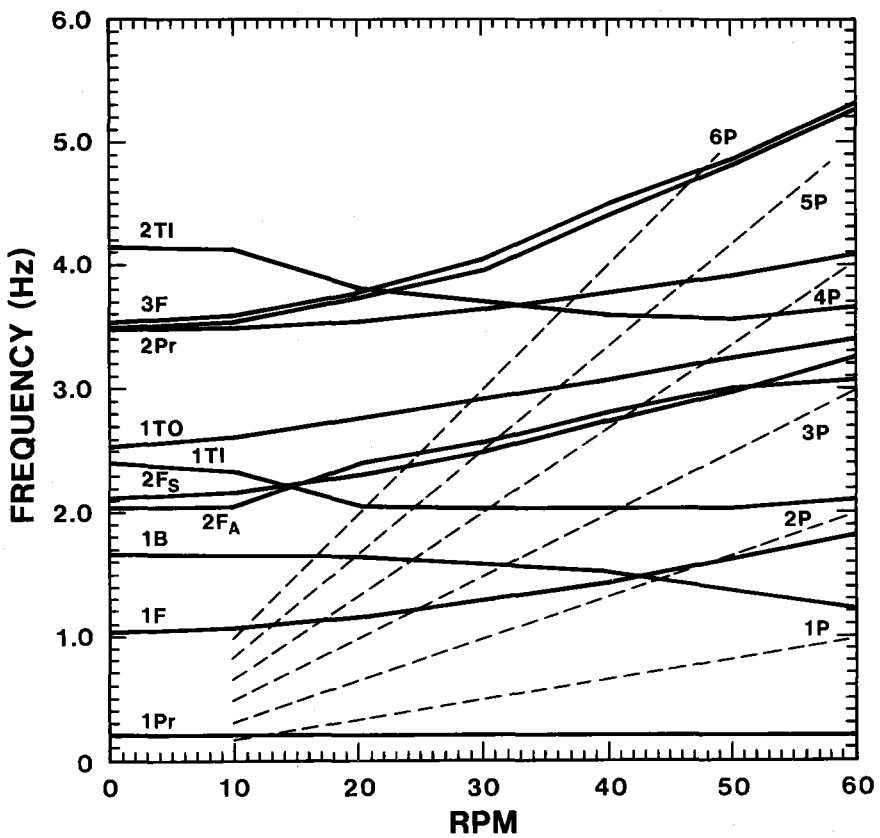

Fig. 7. Rotor Fanplot - Brakes Disengaged

The turbine has operated at rotation rates from 6 to 40 rpm in winds up to 17 mps. Time series have been analyzed with the aid of the data acquisition and analysis (DAAS) software (11). This software can plot any segment of a time series, compute the statistical properties of a segment, statistically reduce the data, and perform spectral analyses. A plot of a strain amplitude spectrum for a flatwise gauge at the upper root at 10 rpm is shown in Fig. 8. The first five per-rev peaks and several other peaks that indicate modal frequencies are evident. By plotting these measured modal frequencies at several rotation rates on the predicted fanplot, as shown in Fig. 9, one can track several rotor modes with rpm. The lower frequency modes (below 3 Hz) including the first and second flatwise (1F,2F), the first blade edgewise (1B), the first tower in-plane (1TI), and the second propeller (2Pr), all track along their predicted mode lines very well. The two measured first flatwise modal frequencies are either the antisymmetric and symmetric modes, which normally vibrate at the same frequency, or the two blades vibrating at slightly different frequencies. The first tower out-of-plane (1TO) does not show up in any of the many spectral plots examined thus far. The first blade edgewise mode (1B) was underpredicted by 5% at zero rpm, but above 25 rpm the observed and predicted frequencies coincide. The first blade edgewise crossing of the 3P line shows up as a larger spike in the spectra of lead-lag gauges at 32 rpm. The stresses are not high in this region in low winds, but significantly increase in winds above 13 mps. The first tower in-plane mode (1TI) tracks well except in the region where it crosses the second flatwise modes. An excitation of this tower in-plane mode begins around 39.5 rpm, and the response is still increasing at 40 rpm. This is due to the 3P crossing predicted at 40.5 rpm. The tower-in-plane excitation which includes blade edgewise motion causes significant lead-lag RMS stresses.

CENTRIFUGAL STRESSES

Figure 10 is a time series record that includes an upper root, flatwise-bending strain gauge and turbine rotation speed. Since the gauges are zeroed before testing, the mean stresses are due solely to centrifugal effects. As the rpm is increased from 0 to 40 rpm, there is an increase in blade bending stresses due to growing centrifugal loading. By averaging each flatwise strain gauge for 40 seconds at each rpm, centrifugal stresses are determined for comparison to analytical results. The increase of centrifugal stresses with higher rpm continues to offset the bending stresses due to gravity until the mean stresses are minimized at 37.5 rpm (the design troposkien rpm).

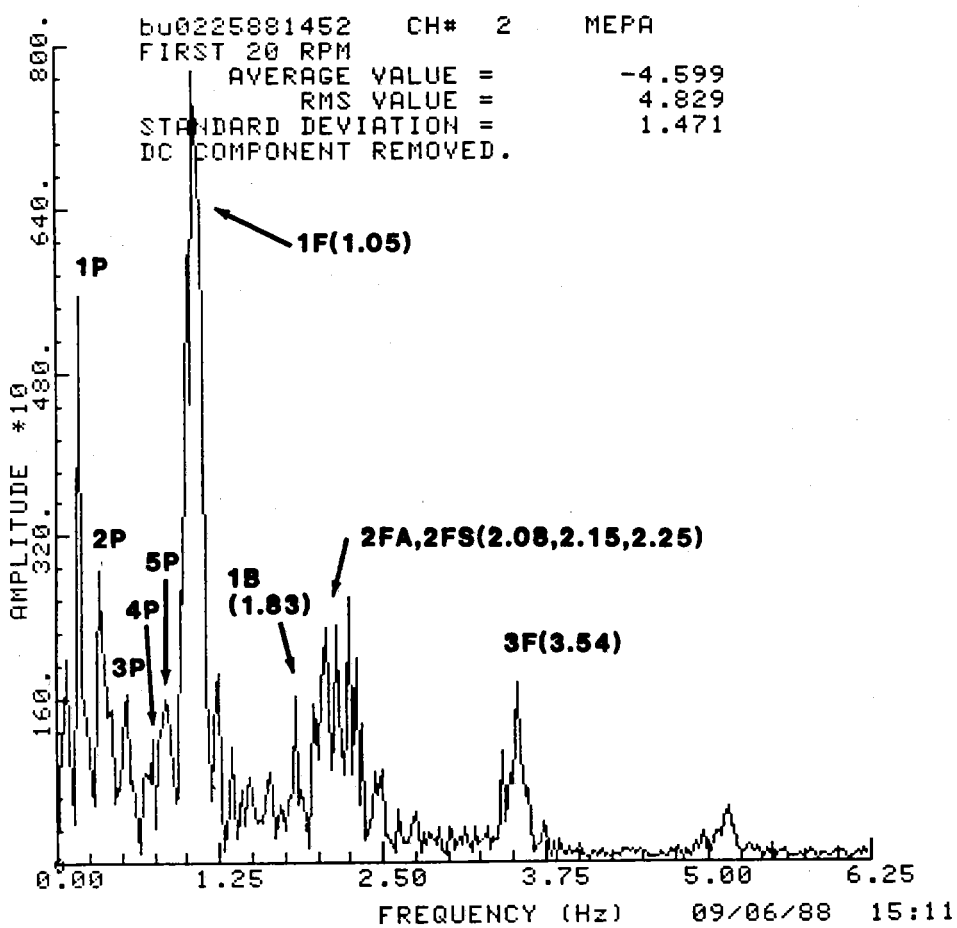

Fig. 8. Strain Amplitude Spectrum at 10 RPM

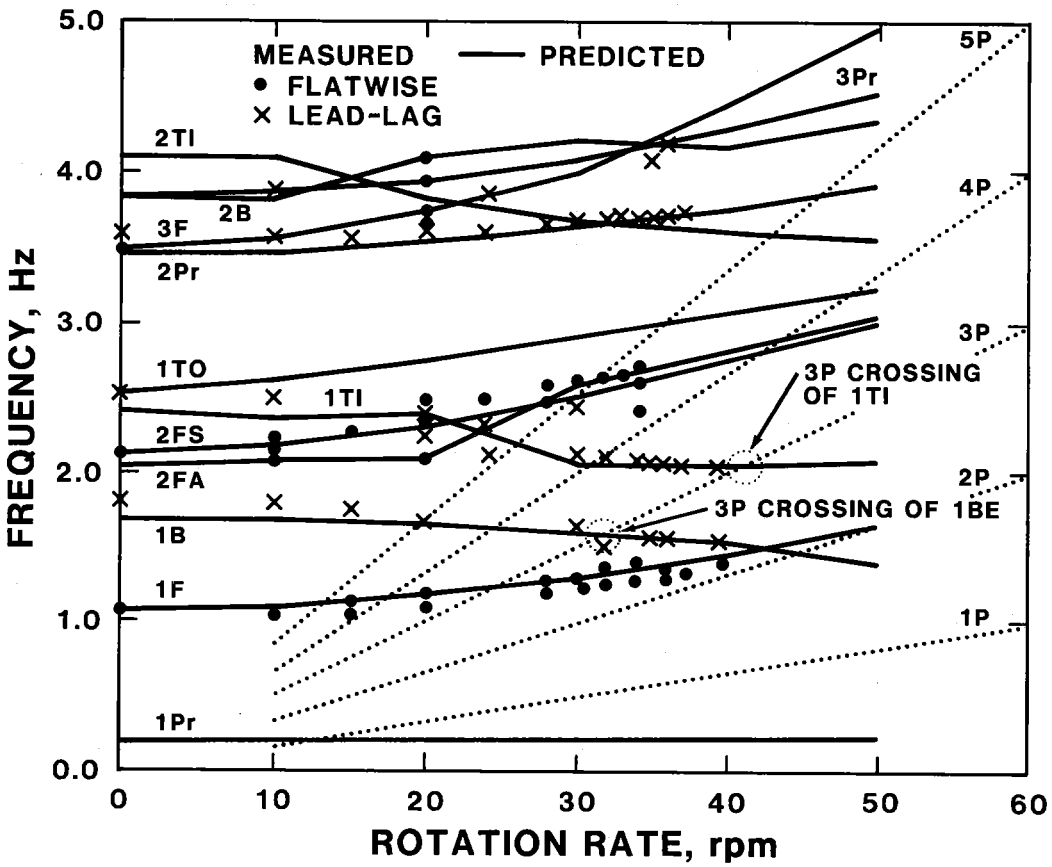

Fig. 9. Rotating Modal Frequencies - Measured vs. Predicted

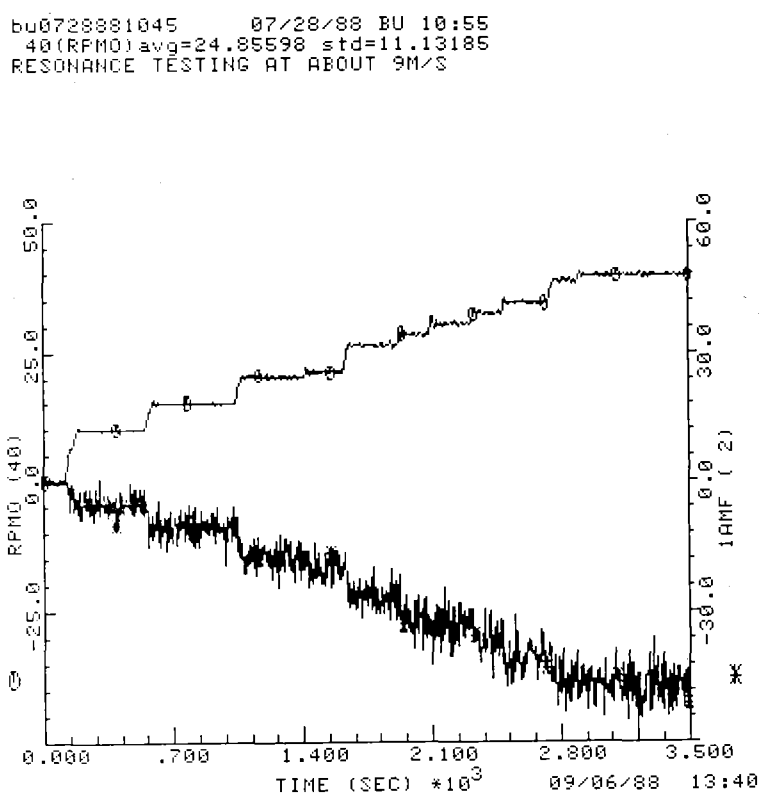

Fig. 10. Upper Root Flatwise Stress vs. RPM

Figures 11 and 12 show a comparison of the measured flatwise centrifugal bending stresses at 28 and 40 rpm to those determined analytically. The stresses along the blade from top to bottom are plotted left to right on the x-axis. There is excellent agreement between the measured and predicted values. Comparisons have also been made at 10,15,20,32,and 36 rpm, and similar agreement is observed.

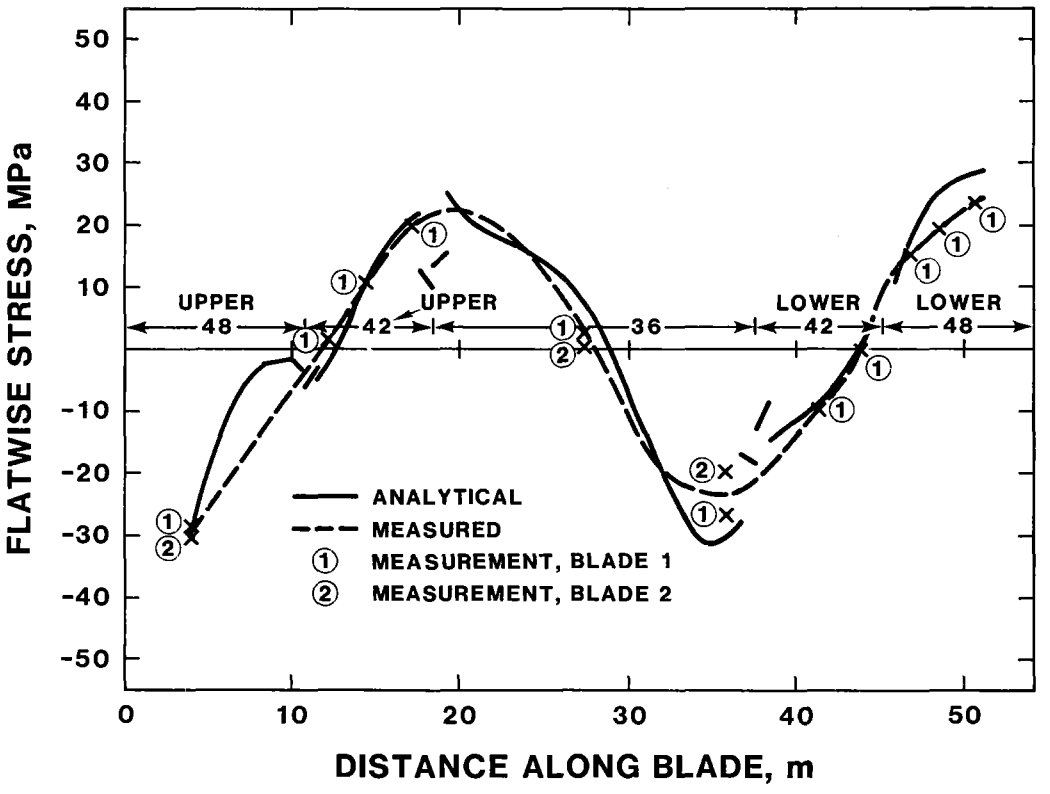

Fig. 11. Centrifugal Stress Distribution at 28 RPM

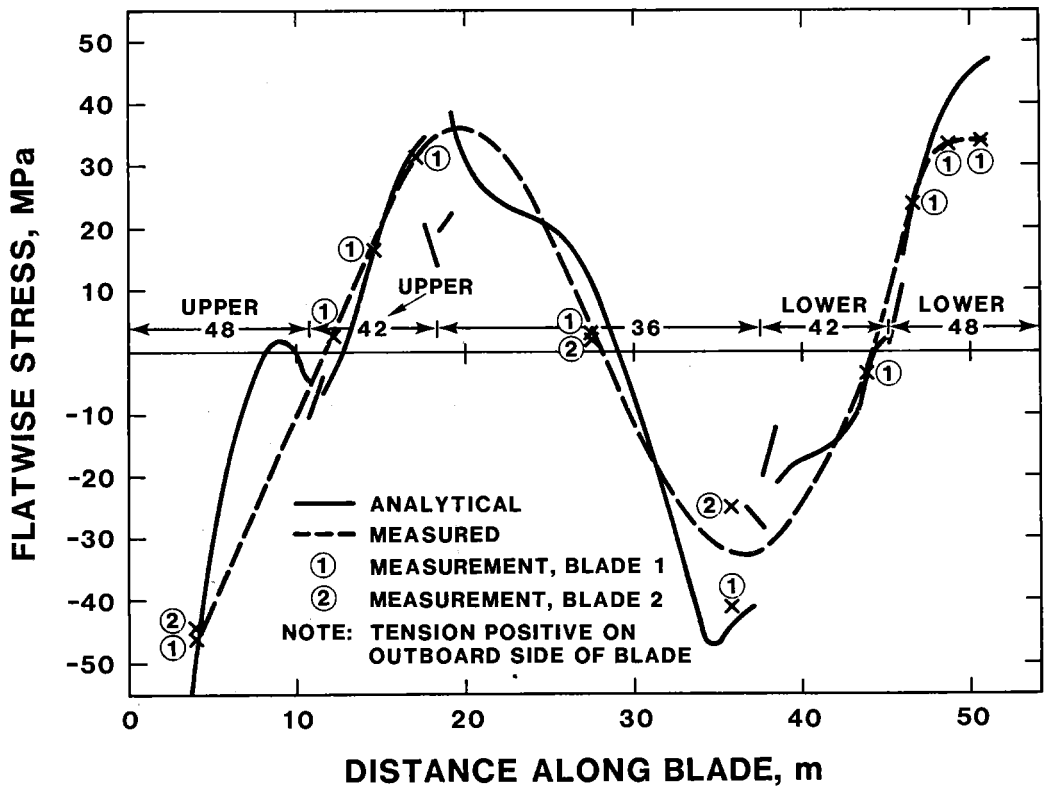

Fig. 12. Centrifugal Stress Distribution at 40 RPM

OPERATING STRESSES

Standard deviations of stress time histories for all recorded channels were computed for segments of data at various rotation rates and wind speeds. This information was used during the resonance surveys for diagnostic purposes (qualitative only) to determine the presence and severity of resonances. It requires hours of time series records at each rpm of interest when using the Method of Bins to obtain quantitative operating stress response and turbine performance as a function of wind speed. Sufficient averaged data are now becoming available for comparisons to predictions.

SUMMARY

At this early stage of testing, the turbine is responding structurally as expected. Predicted gravity stresses compare very well to measured values over most of the blade. Small adjustments to the model's blade attachment angles, if justified, may result in even better agreement.

The first guy cable mode was measured at its design frequency. Interaction between the heavy cable attachment hardware and the cables causes the second and higher modes to be lower than predicted because of the design assumption of a uniform cable mass distribution. A more exact cable model that includes the proper mass distribution of the attachment hardware has recently been developed. The second cable mode appears to become excited at two per-rev around 37 rpm.

A modal test was performed on the stationary rotor. The measured modal frequencies were compared to analytical predictions with excellent results. Rotating modal frequencies obtained from strain amplitude spectra also agree closely with predicted values.

Measured centrifugal stresses have been compared to analytical predictions at several rotation rates, and again, agreement has been excellent.

The close agreement between measured and predicted modal frequencies and mean stresses indicates that the finite element model accurately represents the 34-m Test Bed structure.

REFERENCES

1. Stephenson, W. A., "Test Plan for the 34 Meter Vertical Axis Wind Turbine Test Bed Located at Bushland, Texas," SAND86-1623, Sandia National Laboratories, Albuquerque, NM, December 1986.

2. Akins, R. A., "Performance Evaluation of Wind Energy Conversion Systems Using the Method of Bins - Current Status," SAND77-1375, Sandia National Laboratories, Albuquerque, NM, March 1978.

3. Klimas, P. C., "Tailored Airfoils for Vertical Axis Wind Turbines," SAND84-1062, Sandia National Laboratories, Albuquerque, NM, November 1984.

4. Ashwill, T. D. and Leonard, T. M., "Developments in Blade Shape Design for a Darrieus Vertical Axis Wind Turbine," SAND86-1085, Sandia National Laboratories, Albuquerque, NM, September 1986.

5. Ashwill, T. D., "Structural Design and Fabrication of the Sandia 34-Meter Vertical Axis Wind Turbine," Proceedings of the 1987 ASME-JSME Solar Energy Conference, Honolulu, HI, March 1987.

6. Carne, T. G., Lobitz, D. W., Nord, A. R., Watson, R. A., "Finite Element Analysis and Modal Testing of a Rotating Wind Turbine," SAND82-0345, Sandia National Laboratories, Albuquerque, NM, October 1982.

7. Lobitz, D. W., and Sullivan, W. N., "Comparison of Finite Element Predictions and Experimental Data for the Forced Response of the DOE 100 kW Vertical Axis Wind Turbine," SAND82-2534. Sandia National Laboratories, Albuquerque, NM, February 1984.

8. Paraschivoiu, I., "Aerodynamic Loads and Performance of the Darrieus Rotor," AIAA Journal of Energy, Volume 6, No. 6, pp 406-412, December 1982.

9. Sutherland, H. J. and Stephenson, W. A., "Rotor Instrumentation Circuits for the Sandia 34-Meter Vertical Axis Wind Turbine," SAND88-1144, Sandia National Laboratories, Albuquerque, NM, July 1988.

10. Carne, T. G., Lauffer, J. P., Gomez, A. J., and Ashwill, T. D., "Model Validation of the Sandia 34-Meter Test Bed Turbine Using Substructured Modal-Testing," Proceedings of the Eighth ASME Wind Energy Symposium, Houston, TX, January 1989.

11. Berg, D., Rumsey, M., Gallo, L., and Burwinkle, D., "Data Acquisition and Analysis System for the Sandia 34-Meter Vertical Axis Wind Turbine, Proceedings of the Seventh ASME Wind Symposium, New Orleans, LA., January 1988.

DISTRIBUTION:

Advanced Alternative Energy
Solutions
Attn: Ugur Ortabasi
5673 W. Las Positas Boulevard
Suite 205
P.O. Box 5246
Pleasanton, CA

Alcoa Technical Center (5)
Aluminum Company of America
Attn: D. K. Ai
J. T. Huang
J. R. Jombock
M. Klingensmith
J. L. Prohaska
Alcoa Center, PA 15069

Alternative Sources of Energy
Attn: L. Stoiaken
Milaca, MN 56353

Amarillo College
Attn: E. Gilmore
Amarillo, TX 79100

The American Wind Energy Association
1730 N. Lynn Street, #610
Arlington, VA 22209

Roger J. Austin
Hydro-LIFT Systems
125 Catron Drive
Reno, NV 89512

Dr. A. S. Barker
Trinity Western
7600 Glover Road
Langley, BC
CANADA V3A 4R9

Battelle-Pacific Northwest
Laboratory
Attn: L. Wendell
P.O. Box 999
Richland, WA 99352

Bechtel Group, Inc.
Attn: B. Lessley
P.O. Box 3965
San Francisco, CA 94119

Dr. George Bergeles
Dept. of Mechanical Engineering
National Technical University
42, Patission Street
Athens, GREECE

Ir. Jos Beurskens
Programme Manager for
Renewable Energies
Netherlands Energy Research
Foundation ECN
Westerduinweg 3
P.O. Box 1
1755 ZG Petten (NH)
The Netherlands

Bonneville Power Administration
Attn: N. Butler
P.O. Box 3621
Portland, OR 97208

Canadian Standards Association
Attn: T. Watson
178 Rexdale Blvd.
Rexdale, Ontario, M9W 1R3
CANADA

Monique Carpentier
Energy, Mines and Resources
Renewable Energy Branch
460 O'Connor St.
Ottawa, Ontario
CANADA K1A OE4

Professor V. A. L. Chasteau
School of Engineering
University of Auckland
Private Bag
Auckland, NEW ZEALAND

W. H. Cherry
4547 Province Line Road
Princeton, NJ 08540

Colorado State University
Dept. of Civil Engineering
Attn: R. N. Meroney
Fort Collins, CO 80521

Commonwealth Electric Co.
Attn: D. W. Dunham
Box 368
Vineyard Haven, MA 02568

M. M. Curvin
11169 Loop Road
Soddy Daisy, TN 37379

Alcir de Faro Orlando
Pontificia Universidade Catolica-PUC/Rj
Mechanical Engineering Department
R. Marques de S. Vicente 225
Rio de Janeiro, BRAZIL

Department of Economic Planning and Development
Barrett Building
Attn: G. N. Monsson
Cheyenne, WY 82002

Beatrice de Saint Louvent
Etablissement d'Etudes et de Recherches Meteorologigues
77 Rue de Serves
92106 Boulogne-Billancourt Cedex
FRANCE

Otto de Vries
National Aerospace Laboratory
Anthony Fokkerweg 2
Amsterdam 1017
THE NETHERLANDS

DOE/ALO/ETWMD
Attn: G. P. Tennyson
Albuquerque, NM 87115

DOE/ALO
Energy Technology Liaison Office
NGD
Attn: Capt. J. L. Hanson, USAF
Albuquerque, NM 87115

DOE Headquarters (5)
Wind/Oceans Technologies Division
Attn: L. J. Rogers
P. R. Goldman
1000 Independence Avenue
Washington, DC 20585

J. B. Dragt
Nederlands Energy Research Foundation
(E.C.N.)
Physics Department
Westerduinweg 3 Petten (NH)
THE NETHERLANDS

Electric Power Research Institute
Attn: J. R. Birk
E. A. DeMeo
3412 Hillview Avenue
Palo Alto, CA 94304

George Elliot, Manager
National Wind Turbine Centre
Department of Trade and Industry
National Engineering Laboratory
East Kilbride
Glasgow G75 OQU
Scotland

John Ereaux
RR No. 2
Woodbridge, Ontario L4L 1A6
CANADA

Dr. Norman E. Farb
10705 Providence Drive
Villa Park, CA 92667

FloWind Corporation
Attn: L. Schienbein
1183 Quarry Lane
Pleasanton, CA 94566

A. D. Garrad
Garrad Hasson
10 Northampton Square
London EC1M 5PA
UNITED KINGDOM

H. Gerardin
Mechanical Engineering Department
Faculty of Sciences & Engineering
Universite Laval-Quebec, G1K 7P4
CANADA

Dr. I. J. Graham
Southern University
Dept. of Mechanical Engineering
P.O. Box 9445
Baton Rouge, LA 70813-9445

R. T. Griffiths
University College of Swansea
Dept. of Mechanical Engineering
Singleton Park
Swansea, SA2 8PP
UNITED KINGDOM

Helion, Inc.
Attn: J. Park, President
Box 445
Brownsville, CA 95919

Indal Technologies, Inc.
Attn: V. Lacey
3570 Hawkestone Road
Mississauga, Ontario
CANADA L5C 2V8

Institut de Recherche d'Hydro-Quebec
Attn: Bernard Masse
1800, Montee Ste-Julie
Varennes, Quebec, JOL 2P.O.
CANADA

Iowa State University
Agricultural Engineering
Attn: L. H. Soderholm
Room 213
Ames, IA 50010

K. Jackson
Dynamic Design
123 C Street
Davis, CA 95616

M. Jackson
McAllester Financial
1816 Summit
W. Lafayette, IN 47906

Leif G. Johansen
Vice President of Operations
Cannon Energy Corporation
P.O. Box 1457
Tehachapi, CA 93561

KW Control Systems, Inc.
Attn: R. H. Klein
RD#4, Box 914C
South Plank Road
Middletown, NY 10940

Kaiser Aluminum and Chemical
Sales, Inc.
Attn: A. A. Hagman
14200 Cottage Grove Avenue
Dolton, IL 60419

Kaiser Aluminum and Chemical
Sales, Inc.
Attn: D. D. Doerr
6177 Sunol Blvd.
P.O. Box 877
Pleasanton, CA 94566

Kansas State University
Electrical Engineering Department
Attn: Dr. G. L. Johnson
Manhattan, KS 66506

R. E. Kelland
The College of Trades & Technology
P.O. Box 1693
Prince Philip Drive
St. John's, Newfoundland, AlC 5P7
CANADA

Kinetics Group, Inc.
Attn: J. Sladky, Jr.
P.O. Box 1071
Mercer Island, WA 98040

L. K. Liljergren
120 East Penn Street
San Dimas, CA 71773

L. Liljidahl
Building 005, Room 304
Barc-West
Beltsville, MD 20705

Olle Ljungstrom
FFA, The Aeronautical Research
Institute
Box 11021
S-16111 Bromma, SWEDEN

Robert Lynette
R. Lynette & Assoc., Inc.
15042 NE 40th Street
Suite 206
Redmond, WA 98052

David Malcolm
Lavalin Engineers, Inc.
Atria North - Phase 2
2235 Sheppard Avenue East
Willowdale, Ontario M25 5A6
CANADA

Massachusetts Institute of
Technology
Attn: Professor N. D. Ham
W. L. Harris, Aero/Astro
Dept.
77 Massachusetts Avenue
Cambridge, MA 02139

Brian McNiff
Engineering Consulting Services
55 Brattle Street
So. Berwick, ME 03908

Michigan State University
Division of Engineering Research
Attn: O. Krauss
East Lansing, MI 48825

Alan H. Miller
10013 Tepopa Drive
Oakdale, CA 95361

Napier College of Commerce
and Technology
Tutor Librarian,
Technology Faculty
Colinton Road
Edinburgh, EH10 5DT
ENGLAND

National Rural Electric
Cooperative Assn.
Attn: Wilson Prichett, III
1800 Massachusetts Avenue, NW
Washington, DC 20036

Natural Power, Inc.
Attn: Leander Nichols
New Boston, NH 03070

New Mexico Engineering
Research Institute (2)
Attn: G. G. Leigh
D. Morrison
Campus P.O. Box 25
Albuquerque, NM 87131

Ohio State University
Aeronautical & Astronautical Dept.
Attn: Professor G. Gregorek
2300 West Case Road
Columbus, OH 43220

Oklahoma State University
Mechanical Engineering Dept.
Attn: D. K. McLaughlin
Stillwater, OK 76074

Oregon State University
Mechanical Engineering Dept.
Attn: R. E. Wilson
Corvallis, OR 97331

Debby Oscar
Massachusetts Institute of
Technology
77 Massachusetts Ave.
Room 1-303
Cambridge, MA 02139

Pacific Gas & Electric Co.
Attn: T. Hillesland
J. J. Iannucci
W. J. Steeley
3400 Crow Canyon Road
San Ramon, CA 94583

Ion Paraschivoiu
Dept. of Mechanical Engineering
Ecole Polytecnique
CP 6079
Succursale A
Montreal, Quebec
CANADA H3C 3A7

Jacques Plante
Shawinigan Consultants, Inc.
620 Dorchester Blvd. West
Montreal, Quebec
CANADA H3B 1N8

Public Service Co. of New Hampshire
Attn: D. L. C. Frederick
1000 Elm Street
Manchester, NH 03105

Public Service Co. of New Mexico
Attn: M. Lechner
P.O. Box 2267
Albuquerque, NM 87103

Dr. R. Ganesh Rajagopalan,
Asst. Prof.
Aerospace Engineering Department
Iowa State University
404 Town Engineering Bldg.
Ames, IA 50011

R. Rangi (2)
Low Speed Aerodynamics Laboratory
NRC-National Aeronautical
Establishment
Montreal Road
Ottawa, Ontario, K1A 0R6
CANADA

RANN, Inc.
Attn: A. J. Eggers, Jr.
260 Sheridan Ave., Suite 414
Palo Alto, CA 94306

Mr. Bent Rasmussen
Overgade 14
DK-7000 Fredericia
DENMARK

Markus G. Real, President
Alpha Real Ag
Feldeggstrasse 89
CH 8008 Zurich
Switzerland

Reynolds Metals Company
Mill Products Division
Attn: G. E. Lennox
6601 West Broad Street
Richmond, VA 23261

R. G. Richards
Atlantic Wind Test Site
P.O. Box 189
Tignish P.E.I., COB 2BO
CANADA

Riso National Laboratory
Attn: Troels Friis Pedersen
Helge Petersen
Peter Hauge Madsen
Postbox 49
DK-4000 Roskilde
DENMARK

H. M. Romanowitz, P. E.
Oak Creek Energy Systems, Inc.
P.O. Box 469
Tehachapi, CA 93561

Dr. Ing. Hans Ruscheweyh
Institut fur Leichbau
Technische Hochschule Aachen
Wullnerstrasse 7
FEDERAL REPUBLIC OF GERMANY

Gwen Schreiner
Librarian
National Atomic Museum
Albuquerque, NM 87185

Arnan Seginer
Professor of Aerodynamics
Technion-Israel Institute of
Technology
Aeronautical Engineering Dept.
Haifa
ISRAEL

Mr. Farrell Smith Seiler, Editor
Wind Energy News Service
P.O. Box 4008
St. Johnsbury, VT 05819

David Sharpe
Dept. of Aeronautical Engineering
Queen Mary College
Mile End Road
London, E1 4NS
UNITED KINGDOM

Kent Smith
Instituto Technologico Costa Rica
Apartado 159 Cartago
COSTA RICA

Solar Energy Research Institute
Attn: R. W. Thresher
1617 Cole Boulevard
Golden, CO 80401

Bent Sorenson
Roskilde University Center
Energy Group, Bldg. 17.2
IMFUFA
P.O. Box 260
DK-400 Roskilde
DENMARK

Peter South
ADECON
6535 Millcreek Dr., Unit 67
Mississauga, Ontario
CANADA L5N 2M2

Southern California Edison
Research & Development Dept.
Room 497
Attn: R. L. Scheffler
P.O. Box 800
Rosemead, CA 91770

G. Stacey
The University of Reading
Department of Engineering
Whiteknights, Reading, RG6 2AY
ENGLAND

Stanford University
Dept. of Aeronautics and
Astronautics Mechanical Engr.
Attn: Holt Ashley
Stanford, CA 94305

Dr. Derek Taylor
Alternative Energy Group
Walton Hall
Open University
Milton Keynes, MK7 6AA
UNITED KINGDOM

Texas Tech University
Mechanical Engineering Dept.
Attn: J. W. Oler
P.O. Box 4289
Lubbock, TX 79409

Walter V. Thompson
410 Ericwood Court
Manteca, CA 95336

K. J. Touryan
P.O. Box 713
Indian Hills, CO 80454

Tulane University
Dept. of Mechanical Engineering
Attn: R. G. Watts
New Orleans, LA 70018

J. M. Turner Technologies, Inc.
Attn: Eric N. Hinrichsen
P.O. Box 1058
Schenectady, NY 12301-1058

US WindPower
Attn: W. E. Holley
G. M. McNerney
Suite 3050
400 West Cummings Park
Woburn, MA 01803

USDA
Agricultural Research Service
Southwest Great Plains Research
Center
Attn: Dr. R. N. Clark
Bushland, TX 79012

United Engineers and
Constructors, Inc.
Attn: A. J. Karalis
P.O. Box 8223
Philadelphia, PA 19101

Universal Data Systems
Attn: C. W. Dodd
5000 Bradford Drive
Huntsville, AL 35805

University of California
Institute of Geophysics
and Planetary Physics
Attn: Dr. P. J. Baum
Riverside, CA 92521

University of Colorado
Dept. of Aerospace
Engineering Sciences
Attn: J. D. Fock, Jr.
Boulder, CO 80309

University of Massachusetts
Mechanical and Aerospace
Engineering Dept.
Attn: Dr. D. E. Cromack
Amherst, MA 01003

University of Oklahoma
Aero Engineering Department
Attn: K. Bergey
Norman, OK 73069

University of Sherbrooke
Faculty of Applied Science
Attn: A. Laneville
P. Vittecoq
Sherbrooke, Quebec, J1K 2R1
CANADA

The University of Tennessee
Dept. of Electrical Engineering
Attn: T. W. Reddoch
Knoxville, TN 37916

W. A. Vachon
W. A. Vachon & Associates
P.O. Box 149
Manchester, MA 01944

Dirk Vandenberghe
State Univ. of Ghent
St. Pietersniewstraat 41
9000 Ghent
BELGIUM

Washington & Lee University
Attn: Dr. R. E. Akins
P.O. Box 735
Lexington, VA 24450

Washington State University
Dept. of Electrical Engineering
Attn: F. K. Bechtel
Pullman, WA 99163

West Texas State University
Government Depository Library
Number 613
Canyon, TX 79015

West Texas State University
Department of Physics
Attn: V. Nelson
P.O. Box 248
Canyon, TX 79016

West Virginia University
Dept. of Aero Engineering
Attn: R. Walters
1062 Kountz Avenue
Morgantown, WV 26505

D. Westlind
Central Lincoln People's
Utility District
2129 North Coast Highway
Newport, OR 97365-1795

Wichita State University
Aero Engineering Department (2)
Attn: M. Snyder
W. Wentz
Wichita, KS 67208

Wind Power Digest
Attn: Michael Evans
P.O. Box 700
Bascom, OH 44809

400	R. C. Maydew
1520	L. W. Davison
1522	R. C. Reuter, Jr.
1522	D. W. Lobitz
1522	E. D. Reedy
1523	J. H. Biffle
1524	C. R. Dohrmann
1524	D. R. Martinez
1550	C. W. Peterson
1552	J. H. Strickland
1556	G. F. Homicz
3141	S. A. Landenberger (5)
3151	W. I. Klein (3)
3154-1	C. L. Ward (8)
	For DOE/OSTI (Unlimited

3161	P. S. Wilson
6000	D. L. Hartley
6200	V. L. Dugan
6220	D. G. Schueler
6225	H. M. Dodd (50)
6225	T. D. Ashwill
6225	D. E. Berg
6225	T. C. Bryant
6225	M. E. Ralph
6225	D. C. Reda
6225	M. A. Rumsey
6225	L. L. Schluter
6225	W. A. Stephenson
6225	H. J. Sutherland
6225	P. S. Veers
7544	D. O. Smallwood
7544	T. G. Carne
7544	J. Lauffer
8524	J. R. Wackerly

☆ U.S. GOVERNMENT PRINTING OFFICE: 1990—773-118/20045